molecular pharmaceutics

ARTICLE

pubs.acs.org/molecularpharmaceutics

Cytotoxicity Screening of Single-Walled Carbon Nanotubes: Detection and Removal of Cytotoxic Contaminants from Carboxylated Carbon Nanotubes

Ruhung Wang,[†] Carole Mikoryak,[‡] Synyoung Li,[‡] David Bushdiecker II,[†] Inga H. Musselman,[†] Paul Pantano,[†] and Rockford K. Draper*[,†,‡,§]

[‡]Department of Molecular & Cell Biology and [†]Department of Chemistry, The University of Texas at Dallas, Richardson, Texas 75080, United States

[§]Medical Nanotechnologies, Inc., 320 Decker Drive, Suite 100, Irving, Texas 75062, United States

ABSTRACT: This study compares the cytotoxicity to cultured mammalian cells of nine different single-walled carbon nanotube (SWNT) products synthesized by a variety of methods and obtained from a cross section of vendors. A standard procedure involving sonication and centrifugation in buffered bovine serum albumin was developed to disperse all the SWNTs in a biocompatible solution to facilitate comparisons. The effect of the SWNTs on the proliferative ability of a standard cell line was then assessed. Of the nine different SWNT materials tested, only two were significantly toxic, and both were functionalized by carboxylation from different vendors. This was unexpected because carboxylation makes SWNTs more water-soluble, which would presumably correlate with better biocompatibility. However, additional purification work demonstrated that the toxic material in the carboxylated SWNT preparations could be separated from the SWNTs by filtration. The filtrate that contained the toxic activity also contained abundant small carbon fragments that had Raman signatures characteristic of amorphous carbon species, suggesting a correlation between toxicity and oxidized carbon fragments. The removal of a toxic contaminant associated with carboxylated SWNTs is important in the development of carboxylated SWNTs for pharmacological applications.

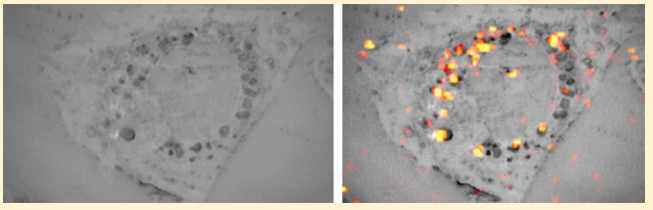

KEYWORDS: carbon nanotubes, nanotoxicology, cytotoxicity, amorphous carbon, carboxylation

INTRODUCTION

Carbon nanotubes (CNTs) come in two basic varieties, single-walled (SWNT) or multiwalled (MWNT). The structural unit of a SWNT is a sheet of sp^2-hybridized graphene rolled into a cylinder. How the sheets are aligned when rolled affects the properties of the resulting SWNTs, which can be either electrically conducting or semiconducting.[1,2] CNTs have useful electronic, optical, and mechanical properties with applications ranging from transistors, to field emission devices, to strong lightweight materials, to pharmacology and nanomedicine.[3,4] The demand for CNTs is driving an exponential growth in their production, and there are now a large number of companies manufacturing or selling CNTs, which has created challenges. One challenge is that the physical and chemical characterization of CNTs is difficult with the result that there is no standardized quality control across the CNT manufacturing industry.[5,6]

A second challenge is what impact CNTs may have on human and environmental health. There is a large literature and unresolved debate on whether CNTs of different types are toxic using a variety of *in vitro* and small animal models (for recent reviews, see refs 7−11). There are several crucial factors contributing to the problem of assessing CNT toxicity. One is the physical purity of the material. Some, but not all, CNT synthetic methods use iron catalysts, and iron is well-known to be toxic because it generates reactive oxygen species. Therefore, it is essential to test for and remove toxic metals from CNT preparations in order to assess the inherent toxicity of CNTs. A second important factor is debundling and dispersal of CNTs using a dispersant that itself is not toxic. The surface of pristine CNTs is hydrophobic, which causes them to aggregate in aqueous solution so the behavior of individual CNTs is difficult to study. Moreover, the hydrophobic surface of CNTs can nonspecifically bind nutrients necessary for cell growth, leading to indirect toxic effects.[12] Another important factor is whether the CNT surface has been covalently functionalized. Functionalization can change the surface chemistry and dispersal properties of the CNTs, which may affect toxicity. An additional confounding factor is the large number of CNT vendors whose product descriptions are similar yet whose CNT products are very different. Also, different lots of the same material from a given vendor may vary.

The outcome of toxicity testing also depends on what model system is investigated and on what toxicity assay is used. There is

Received: March 20, 2011
Accepted: June 20, 2011
Revised: June 3, 2011
Published: June 20, 2011

Table 1. Properties of SWNT Material Provided by Manufacturers and Analysis of Laboratory-Prepared SWNT Dispersions

	properties of SWNT powders provided by manufacturers						analysis of SWNT dispersions	
				purity				
SWNT product	synthetic method	metal catalyst	purification/functionalization	% carbon	% SWNTs	SWNT diam (nm)	concn[a] (μg/mL)	Raman D/G ratio[b]
A1	CVD	Co/Mo	purified	>90	≥70	0.7−1.3	230 ± 10	0.15 ± 0.04
A2	CVD	Co/Mo	purified	>90	≥77	0.7−0.9	301 ± 63	0.11 ± 0.03
A3	CVD	Co/Mo	purified	>90	≥77	0.7−1.1	258 ± 31	0.08 ± 0.01
B1	CVD	Fe	raw	>65	NA[c]	0.8−1.2	401 ± 55	0.07 ± 0.00
C1	arc discharge	Ni/Y	raw	40−60	NA	~1.4	241 ± 29	0.05 ± 0.01
C2	arc discharge	Ni/Y	purified	>90	NA	~1.4	289 ± 41	0.02 ± 0.01
C3	arc discharge	Ni/Y	carboxylated	>90	NA	~1.4	786 ± 61	0.24 ± 0.04
D1	CVD	Fe/Mo	purified	>95	NA	~1.5	229 ± 80	0.13 ± 0.03
D2	CVD	Fe/Mo	carboxylated	>95	NA	~1.5	919 ± 33	0.39 ± 0.03

[a] Mean concentrations of total carbon species in SWNT dispersions were determined using the SDS−PAGE method (see Materials and Methods); the standard deviations represent at least $n = 3$ independent measurements. [b] The D/G quality factor was determined using Raman spectroscopy with 532 nm laser excitation (where D represents the area of the D-band from 1250 to 1450 cm^{-1} and G represents the area of the G-band from 1450 to 1650 cm^{-1}); the standard deviations represent at least $n = 6$ independent measurements. [c] NA, not available.

evidence that raw nonfunctionalized CNTs in the lungs of test animals result in a toxic pathology.[8,13,14] This is important information if the objective is to determine the risk of inhaling airborne raw CNT particles, and it is clear that measures to prevent airborne CNTs in the workplace are important. Another valid question is whether CNTs themselves are inherently toxic when presented to cells in an aqueous environment, which could occur by accidental ingestion or as a consequence of pharmacological or therapeutic applications. This paper addresses whether SWNTs produced by a variety of methods and obtained from a cross section of vendors, but dispersed under identical standard conditions, are inherently cytotoxic to cultured cells.

We compared the cytotoxicity of nine different SWNT materials from five different vendors prepared by a variety of synthetic methods. A standard set of protocols was developed to characterize each SWNT material and to disperse the SWNTs by sonication in buffered bovine serum albumin. The effect of the SWNTs on the proliferative ability of a standard cell line was then assessed. For the nine different SWNT materials tested, only two were significantly toxic, and both were functionalized by carboxylation with acids by their vendors. This was unexpected because carboxylation makes SWNTs more water-soluble and should correlate with better biocompatibility and presumably reduced toxicity. However, additional purification work demonstrated that the toxic material could be separated from the SWNTs by filtration; thus, the SWNTs were not the toxic species in the carboxylated SWNT preparations. Interestingly, the filtration fraction that exhibited toxicity also contain small heterogeneous carbon fragments that had Raman signatures characteristic of amorphous carbon species, suggesting a possible correlation between toxicity and fragments of oxidized carbon.

RESULTS

Selection of SWNT Materials and Characterization of Dispersions. Whereas all SWNT manufacturing processes use a carbon feedstock, metal catalysts, and heat, each technique produces a heterogeneous powdered soot that contains different SWNT chiralities, undesirable synthetic byproducts (such as graphitic and amorphous carbon phases), metals, and, in some cases, catalyst support material. As shown in Table 1, the materials chosen for this work represent four of the major commercial SWNT synthetic methods: Ni/Y-catalyzed arc discharge SWNTs, Fe/Mo-catalyzed CVD SWNTs, Fe-catalyzed CVD SWNTs, and Co/Mo-catalyzed CVD SWNTs. The SWNT powders are further classified as raw (as-produced soot removed from the reactor without further processing), purified (refined SWNT material with low chemical functionality), and carboxylated (refined SWNT material with various degrees of carboxyl groups at tube ends and sidewalls).

Scheme 1. Preparation of SWNT Dispersions

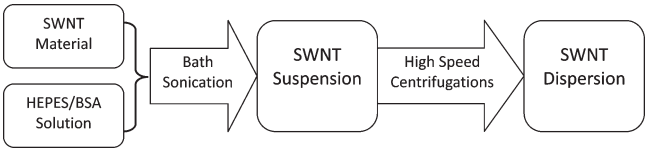

A bath sonication and centrifugation protocol in the presence of 4-(2-hydroxyethyl)-1-piperazineethanesulfonic acid (HEPES) buffer and bovine serum albumin (BSA) was used to process SWNT powders into aqueous SWNT dispersions (Scheme 1). This protocol consistently produced individually dispersed SWNTs with short lengths and effectively removed heavy metal contaminants; most notably, the sub-ppm metal levels of Fe, Ni, Y, Mo, and Co detected in SWNT dispersions by ICP-MS were below toxic levels for each respective metal. Figure 1 shows representative absorption spectra of aqueous SWNT dispersions prepared from each of the nine SWNT powders listed in Table 1. The absorption features observed in each spectrum correspond to the M_{11}, S_{22}, and S_{11} optical transitions of the metallic and semiconducting SWNT structures contained in each dispersion, whereas the nonresonant backgrounds include contributions from the π-plasmon absorptions of both SWNTs and other carbonaceous species present in the purified, aqueous dispersions.[15]

The absorption spectra (Figure 1A) of the SWNT dispersions prepared from the Co/Mo-catalyzed CVD SWNT powders (A1-, A2-, and A3-SWNTs) and from the Fe-catalyzed CVD SWNT

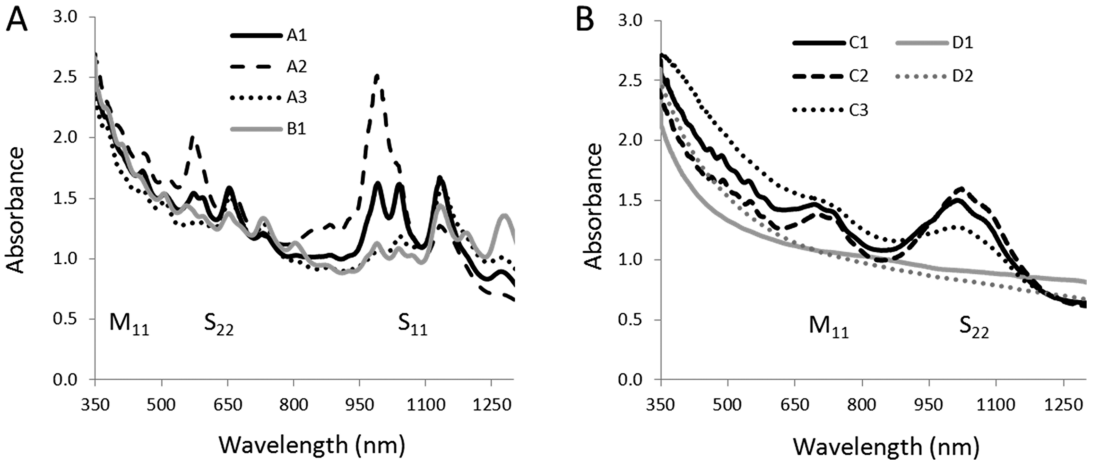

Figure 1. Representative background-corrected absorption spectra of SWNT dispersions prepared from the nine SWNT materials shown in Table 1; the carbon content of all dispersions was 100 μg/mL. (A) Spectra of A1-, A2-, and A3-SWNT dispersions (black lines) prepared from the three purified CVD materials purchased from manufacturer A and the spectrum of B1-SWNT dispersion prepared from the raw CVD material (gray line) purchased from manufacturer B. (B) Spectra of C1-, C2-, and C3-SWNT dispersions (black lines) prepared from raw, purified, and carboxylated electric-arc discharge material purchased from manufacturer C, respectively, and the spectra of D1- and D2-SWNT dispersions prepared from purified and carboxylated CVD material (gray lines) purchased from manufacturer D, respectively. For A1-, A2-, A3- and B1-SWNT dispersions in panel A, and C1-, C2-, and C3-SWNT dispersions in panel B, the M_{11}, S_{22}, and S_{11} labels represent the approximate regions of the first and second interband transitions for metallic and semiconducting SWNT structures.

powder (B1-SWNTs) all display sharp van Hove peaks characteristic of debundled, individually dispersed SWNTs.[16,17] Collectively, these four samples represent a series of aqueous SWNT dispersions that contain primarily semiconducting SWNTs with varying diameters. For example, the most intense optical transitions in the S_{11} spectral region for the A1-SWNTs correspond to (*6,5*), (*7,5*), and (*7,6*) semiconducting SWNTs with diameters ranging from 0.8 to 1.0 nm. The absorption spectra of the SWNT dispersions prepared from the Ni/Y-catalyzed arc discharge SWNT powders (C1-, C2-, and C3-SWNTs) and from the Fe/Mo-catalyzed CVD SWNT powders (D1- and D2-SWNTs) are shown in Figure 1B. C1 (raw soot) and C2 (purified) have broad peaks in the S_{22} spectral region corresponding to overlapping optical transitions from the large number of semiconducting SWNTs that are produced by the electric arc method. The absorption spectrum of D1, made by the catalytic CVD technique, was unexpectedly featureless even though SWNTs made with this technique can have wide diameter distributions with significant overlap of interband transitions.[6] C3, a carboxylated sample, displayed broadened transitions in the S_{22} spectral region as expected for carboxylated material. The other carboxylated sample, D2, had no peaks, which may be indicative of a heavily oxidized SWNT surface.[18]

Raman spectroscopy with 532 nm laser excitation was also used to characterize the SWNT dispersions by calculating a D/G quality factor, where D represents the area of the D-band from 1250 to 1450 cm^{-1} and G represents the area of the G-band from 1450 to 1650 cm^{-1}. For high-quality samples containing fewer defects and less amorphous carbon species the D/G ratio is often below 0.02.[6] As shown in Table 1, the D/G Raman quality factors of SWNT dispersions prepared from the two raw SWNT powders were 0.07 (B1) and 0.05 (C1), and those prepared from the five purified SWNT powders, A1, A2, A3, C2, and D1, ranged from 0.02 to 0.15. These data indicate that the bath sonication/centrifugation process used to generate SWNT dispersions is effective in reducing a variety of undesirable synthetic

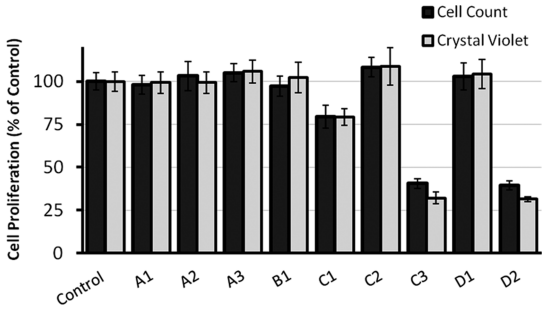

Figure 2. *In vitro* cytotoxicity assessment of various SWNT dispersions on NRK cells. Cultured NRK cells were incubated in media with various SWNT dispersions at 100 μg/mL concentration or in the absence of SWNTs (control) for 3 days. Cytotoxicity was assessed by cell proliferation, quantified by comparing the number of cells or the amount of nucleic acid stained with crystal violet dye. Each bar is the mean of three independent experiments with error bars showing standard deviations.

byproducts from SWNT powders produced by the four different synthetic methods. The D/G Raman quality factors of SWNT dispersions prepared from the two carboxylated SWNT powders were 0.24 (C3) and 0.39 (D2), as expected, because carboxylation by reaction with oxidizing acids can introduce defects into the SWNT lattice that increase the D/G ratio.[19]

***In Vitro* Cytotoxicity Screen of SWNT Dispersions.** Physical characterization of the SWNTs in the previous section determined that the various SWNTs from different vendors represent a spectrum of SWNT purities and types. To determine if there were differences in potential cytotoxic effects among the SWNTs, normal rat kidney cells (NRK, an established cell line) were exposed to 100 μg/mL SWNT dispersions in complete growth medium for three days. Proliferation was then measured directly by counting the number of remaining cells with a Coulter counter, and indirectly using a rapid crystal violet staining assay.[20] Six of the SWNT preparations tested had no effect on

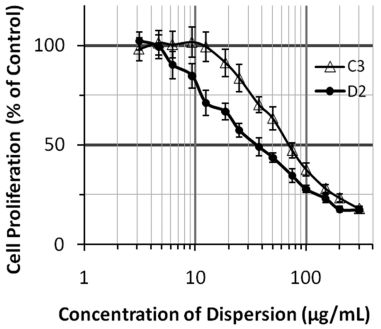

Figure 3. Dose response of two carboxylated SWNT dispersions on NRK cells. Cultured NRK cells were incubated in media with C3- or D2-SWNT dispersions at increasing concentrations from 3 to 300 μg/mL or in the absence of SWNTs (control) for 3 days. Cytotoxicity was determined by measuring the ability of the cells to proliferate, as quantified by the amount of nucleic acid stained with crystal violet dye. Cell proliferation in the presence of SWNT dispersions was compared to the control, which was taken as 100%. Each data point is the mean of three independent experiments, and the error bars show the standard deviations.

cell growth. Raw arc-discharged material C1 mildly depressed proliferation, while C3 and D2 dispersions reduced growth by about 60% (Figure 2). The results with C3 and D2 SWNT dispersions were surprising because they are functionalized by carboxylation to make them more water-soluble and biocompatible.

The effects of the C3 and the D2 SWNT materials on cell proliferation, as a function of concentration in the media, were determined by crystal violet assay after 3 days incubation. The IC50 values of the C3- and D2-SWNT dispersions obtained from three independent experiments were 76.5 $\pm$ 4.9 μg/mL and 41.0 $\pm$ 3.1 μg/mL, respectively (Figure 3). Thus, the toxic effects of the C3 and the D2 SWNT materials on cell proliferation are dose dependent. The IC50 values were also a function of exposure time, decreasing as the time increased (data not shown).

Uptake and Detection of SWNTs in NRK Cells. There are numerous reports that SWNTs can enter cells by endocytosis and accumulate in lysosomes.[21−23] To determine if both the cytotoxic and the noncytotoxic SWNT types accumulated in lysosomes, we studied the uptake and subcellular distribution of C2- and C3-SWNTs by scanning confocal Raman microscopy. NRK cells grown on glass coverslips were incubated in media containing 100 μg/mL C2- or C3-SWNT dispersions for two days at 37 °C. To identify lysosomes, 0.12 M sucrose was added to the medium for the last 24 h of incubation. Sucrose enters lysosomes by fluid phase endocytosis but is not degraded by most cells, which causes the lysosomes to osmotically swell and allows lysosomal vesicles to be identified by light microscopy without staining.[24,25] The cells were washed, fixed with paraformaldehyde, air-dried, and examined by scanning confocal Raman microscopy with a 532 nm laser. The cell-associated SWNTs were detected directly by their Raman signature in the absence of any fluorescent dyes or other labels. Results shown in Figure 4A−C were acquired from NRK cells treated with the C2-SWNT dispersion, and Figure 4D was acquired from cells treated with the carboxylated C3-SWNT dispersion. Figure 4A is an optical image of a fixed NRK cell in a defined 50 × 40 μm area showing the enlarged lysosomal vesicles in the perinuclear region. The same area was scanned by confocal Raman microscopy, and the SWNT G-band signal (1460−1700 cm^{-1}) at every pixel was

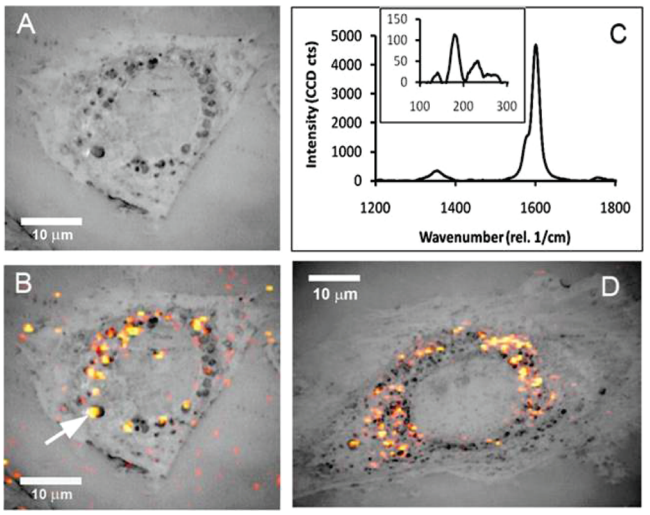

Figure 4. Label-free detection of noncarboxylated C2-SWNTs and carboxylated C3-SWNTs inside NRK cells by confocal Raman microscopy. NRK cells grown on glass coverslips were incubated in media with C2- or C3-SWNT dispersions at a concentration of 100 μg/mL for 48 h with the addition of 0.12 M sucrose during the last 24 h. The cells were washed, fixed with paraformaldehyde, air-dried, and examined by confocal Raman microscopy with a 532 nm laser. (A) Optical image of a NRK cell incubated with C2-SWNT dispersion. (B) Optical image from (A) was overlaid with a Raman scan of the same area where the SWNT G-band signal (1460−1700 cm^{-1}) at every pixel was mapped using a thermal color scale with yellow being the highest intensity. (C) Background-corrected Raman spectrum taken from one pixel in the hot spot indicated by the arrow in (B). The inset shows the enlarged RBM region of the spectrum. (D) Optical image of a cell incubated with C3-SWNT dispersion was overlaid with a Raman scan of the same area to show colocalization of the SWNT Raman signals with the vesicles.

mapped using a thermal color scale with yellow being the highest intensity. Figure 4B shows the optical image of the scanned area overlaid with the Raman scan image. It is evident that the SWNT Raman signature localizes in the vicinity of the swollen lysosomes. Figure 4C shows a background-corrected Raman spectrum taken from one pixel in the hot spot that corresponds to an enlarged lysosome, marked by an arrow in Figure 4B. The Raman D/G ratio is very similar to the C2-SWNT dispersion in Table 1, suggesting that there has been no chemical or physical modification of the internalized SWNTs that affects their Raman response. The inset in Figure 4C shows the magnified radial breathing modes of the Raman spectrum (100−300 cm^{-1}). The radial breathing mode Raman signals arise from the tubular SWNT structure and validate unambiguously the direct detection of SWNTs within the cells.[19,26] Cells incubated with the toxic C3-SWNT dispersion were also examined, and an optical image of the cell overlaid with the Raman scan is shown in Figure 4D. In general, no morphological differences were observed among cells treated with either C2- or C3-SWNT dispersions, and both had a similar perinuclear distribution of SWNTs that colocalized with lysosomes. These data suggest that SWNTs from both noncytotoxic and cytotoxic dispersions accumulate in lysosomes of NRK cells.

We then investigated whether the amount of C2- and C3-SWNT materials taken up by cells correlates with cytotoxicity. NRK cells were incubated for 3 days in media containing C2- or C3-SWNT dispersions at 100 μg/mL or in the absence of SWNT

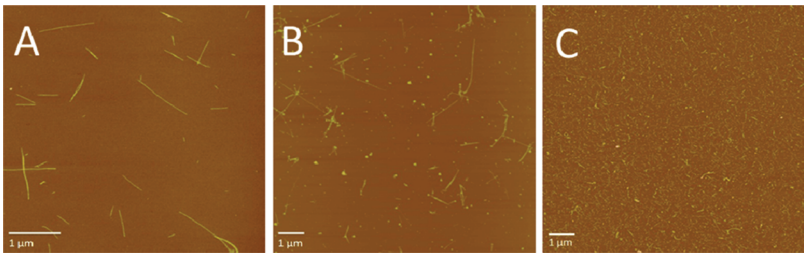

Figure 5. AFM images of noncarboxylated and carboxylated SWNT dispersions. Panel A shows a representative AFM image of the noncarboxylated, nontoxic C2-SWNT dispersion in a HEPES and BSA solution. Panels B and C are representative AFM images of the carboxylated, toxic C3- and D2-SWNT dispersions in water, respectively.

dispersions as a control. After the incubation, the SDS−PAGE method was used to extract and quantify cell-associated SWNTs and related material from cells as previously described by Wang et al.[27] The average amount of C2- or C3-SWNT materials inside a cell was calculated using the amount extracted divided by the total number of cells in a well. The average amount of C2-SWNT material accumulated by cells was 555.6 ± 60.6 fg/cell and that for C3-SWNTs was 548 ± 100.7 fg/cell. This demonstrated that both carboxylated and noncarboxylated SWNT materials accumulated to the same level in cells and that the difference in the cytotoxicity between the two SWNT types cannot be explained by differences in cell uptake.

Detection of Amorphous Carbon Fragments in Carboxylated SWNT Products. The two toxic SWNT materials, C3 and D2, were acid treated by manufacturers to contain 1.5−3.0% and 2−7% carboxylic acid groups, respectively. None of the other SWNT products in this study were intentionally carboxylated. This suggests a possible correlation between toxicity and the carboxylation process. The most common carboxylation technique involves refluxing SWNTs in nitric acid or a nitric/sulfuric acid mixture at high temperature. This treatment carboxylates the SWNTs, but is also well-recognized to produce various oxidized carboxylated amorphous carbon fragments.[28−30] To investigate whether the carboxylated SWNT samples contain small amorphous carbon fragments inherited from the carboxylation process, SWNT dispersions prepared from carboxylated and noncarboxylated materials were examined by atomic force microscopy (AFM). Figures 5A, 5B, and 5C are representative AFM images acquired from C2-, C3-, and D2-SWNT dispersions, respectively. As shown in Figure 5A, the C2-SWNT dispersion contains abundant cylindrical individually dispersed SWNT-like features with an average length of 329 ± 328 nm (n = 203). Unlike the C2-SWNT dispersion, the AFM image of the carboxylated C3-SWNT dispersion (Figure 5B, in H_2O with no surfactant) reveals individually dispersed SWNT-like features along with many small nontubular shaped species. The average length and diameter of the cylindrical features in the C3-SWNT dispersion sample were 149 ± 123 nm and 1.72 ± 0.79 nm (n = 190), respectively. The sizes of the nontubular species in the C3-SWNT dispersion images were measured and were shown to be 39.3 ± 10.6 nm (n = 70) in the longest dimension. The AFM image of the highly carboxylated D2-SWNT dispersion (Figure 5C) shows small nontubular species in greater abundance than in the C3-SWNT dispersion images. Additionally, the lengths of the cylindrical SWNT-like features in 5C are shorter than those in Figure 5A or Figure 5B. These results suggest that carboxylated SWNT samples contain small nontubular species, most likely amorphous carbon fragments stemming from the carboxylation process.

Scheme 2. Detoxification of Carboxylated C3-SWNT Dispersions by Filtration

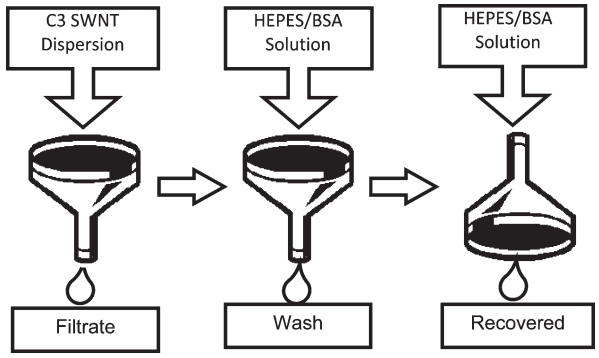

Detoxification of C3-SWNT Dispersion by Filtration. The apparent presence of small amorphous carbon fragments in the two carboxylated SWNT materials suggested that there may be a correlation between toxicity and the small fragments. To test this hypothesis, we purified the toxic C3-SWNT dispersion by filtration through a polyvinylidene fluoride (PVDF) filter membrane with a 0.22 μm pore size, as summarized in Scheme 2, to separate small carbonaceous fragments from SWNTs in the dispersion. The filtrate was collected and the membrane was washed with 5 mL of HEPES/BSA. The material retained on the membrane was then suspended in 3 mL of HEPES/BSA and redispersed for 30 min by sonication.

The SWNTs in the C3 dispersion, the filtrate, and the recovered samples were examined by AFM, and the representative images are shown in Figures 6A, 6B, and 6C, respectively. As shown in Figure 6A, the C3-SWNT dispersion contains abundant SWNT-like cylindrical features and a high background of small nontubular, amorphous fragments. The AFM image of the filtrate sample (Figure 6B) reveals small species of various shapes but no SWNT-like cylindrical features. In contrast, the image of the recovered C3-SWNT dispersion after filtration contained mainly individually dispersed SWNT-like features with very few small, nontubular amorphous fragments (Figure 6C). This demonstrated that most of the small amorphous fragments in the initial C3-SWNT dispersion were separated from the long, cylindrical SWNT-like features by filtration. The filtration approach could not be applied to the D2-SWNT dispersion

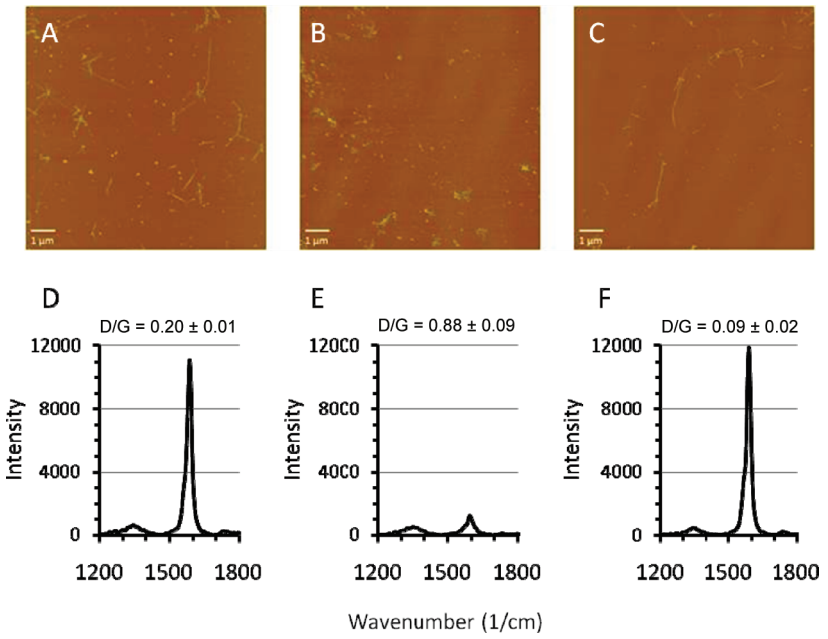

Figure 6. AFM and confocal Raman microscopy analysis of C3-SWNT dispersions before and after filtration. The toxic C3-SWNT dispersion was filtered with a 0.22 μm membrane, the filtrate was collected, and the material retained on the membrane was recovered and redispersed in a HEPES buffered BSA solution (see Scheme 2). Panels A, B, and C are representative AFM images of the C3-SWNT dispersion, the filtrate, and the recovered material, respectively. Panels D, E, and F are Raman spectra of the C3-SWNT dispersion, the filtrate, and the recovered material, respectively. The Raman spectra and the (D/G) quality factor values are the averages of six measurements.

because nearly all the material in the dispersion was too small to be retained on the filter.

The C3-SWNT dispersion, the filtrate, and the recovered samples were then examined by Raman spectroscopy with results shown in Figures 6D, 6E, and 6F, respectively. The strong G-band signals in the Raman spectra acquired from the initial C3-SWNT dispersion and the recovered samples (in Figures 6D and 6F) validate the presence of abundant SWNTs in these samples. As expected, a much smaller G-band signal was present in the Raman spectrum acquired from the filtrate sample which contains far less carbonaceous material (Figure 6E). The Raman D/G quality factor of the C3-SWNT dispersion, the filtrate, and the recovered samples were 0.20 ± 0.01, 0.88 ± 0.09, and 0.09 ± 0.02, respectively. The high Raman D/G ratio of the filtrate sample suggests the abundant presence of amorphous carbon species. The low Raman D/G ratio of the recovered sample indicates that a purified SWNT sample containing mainly dispersed SWNTs can be prepared by a simple filtration process. These results are in agreement with those of AFM analysis. Finally, the recovered sample of intact SWNTs contained 4 atom % of carboxylic acid groups as determined by XPS, demonstrating that it was carboxylated. Together, these findings suggest that the amorphous carbon fragments found in carboxylated SWNT materials can be removed by filtration and that the filtration-purified SWNT dispersion contains mainly intact dispersed carboxylated SWNTs.

Cytotoxicity Assay of the Detoxified C3-SWNT Dispersion. To see if the presence of amorphous carbon fragments correlates with the toxicity observed in the C3-SWNT dispersion, the effects of the initial C3-SWNT dispersion, the filtrate, and the filter-adherent material on cell proliferation were measured using our standard *in vitro* cytotoxicity assay. As described previously in Figure 2, NRK cells were incubated in media containing either

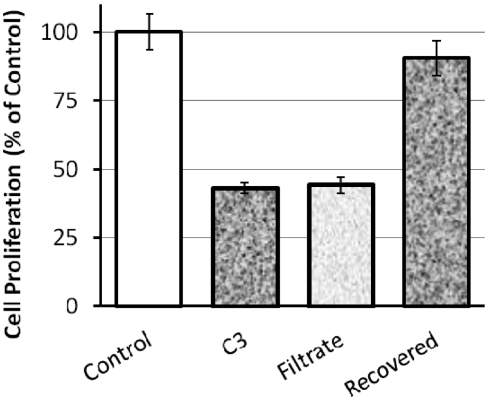

Figure 7. Cytotoxicity assessment of C3-SWNT dispersions before and after filtration. Cultured NRK cells were incubated in media containing either C3-SWNT dispersion (100 μg/mL), the filtrate material (17 μg/mL), or the recovered material (101 μg/mL), or in the absence of SWNTs (control) for 3 days. Cytotoxicity was determined by measuring cell proliferation, as quantified by comparing the amount of nucleic acid stained with crystal violet dye. Each bar in the graph is the mean of three independent experiments with error bars showing the standard deviations.

C3-SWNT dispersion (100 μg/mL), the filtrate (17 μg/mL), or the filter-adherent sample (101 μg/mL), or in media containing no SWNT materials as a control. After three days, relative cell proliferation was compared to that of the untreated control cells (Figure 7). It is apparent that nearly all the cytotoxic materials passed through the membrane with the filtrate and that the SWNTs recovered from the membrane had little cytotoxicity. These results support the hypothesis that the toxicity of carboxylated SWNT preparations results from small amorphous carbon

fragments that can be separated from the nontoxic SWNTs by filtration.

DISCUSSION

Carbon nanotubes of different types produced by different methods, often with proprietary synthetic details, are commercially available from a wide variety of vendors. It is difficult to compare the properties of different materials, even those synthesized by similar methods, based on manufacturer-supplied data sheets because there is no standard set of data available from all manufacturers. Moreover, there is essentially no vendor data available on the toxicity of various CNT types. One objective of the present work was to develop a standard procedure for detecting the potential cytotoxicity of SWNTs produced by different synthetic methods and by different vendors. All of the samples were dispersed in a HEPES-buffered BSA solution using a sonication and centrifugation method to remove metal contaminants and SWNT bundles, providing uniform and stable dispersions at high concentrations for comparison. This method is rapid, can be used to simultaneously prepare multiple samples, dispersed every SWNT material we tested, and is biocompatible with cytotoxicity testing. Spectral characterization of the samples provided results expected for well-dispersed SWNTs, with the exception that optical transitions were absent for the purified D1 material. It is interesting to note that A1, A2, and A3 samples, all having strong optical signals, were made by a CVD method, as was D1, yet the properties were very different. This emphasizes that SWNTs prepared by the same general method but with unique catalysts may be dissimilar depending on synthetic and purification details. It is likely that the absence of absorption peaks in the D1 dispersion is due to the presence of a wide variety of SWNT types with overlapping optical peaks. The absence of peaks in the D2 material is likely because it was made from D1 and was also carboxylated, which broadens optical transitions.

Cytotoxicity was assessed with a standard cell line, NRK cells, by measuring the effect of SWNT dispersions on cell proliferation. It is well-documented that organic dyes used in cell viability assays can interact with SWNTs and interfere with viability results.[31] Therefore, we directly counted cell numbers after three days of growth to measure effects on viability. A rapid crystal violet assay was also used to measure proliferation, and the method was validated by comparing the results to direct cell counting. Only three of the nine SWNT samples showed evidence of cytotoxicity upon exposure of cells to a high concentration of 100 μg/mL. Dispersion C1, representing a raw arc-discharged material, was very mildly cytotoxic with a 20% reduction in proliferation. The most interesting result, however, was that the most cytotoxic SWNT dispersions were both carboxylated, samples C3 and D2, with IC50 values of 76.5 $\pm$ 4.9 μg/mL and 41.0 $\pm$ 3.1 μg/mL, respectively, after an exposure to SWNTs of 3 days. Further work is necessary to determine whether the reduced cell proliferation is the result of a cytotoxic or a cytostatic mechanism. In addition, the IC50 values are a function of exposure time and a lower concentration may cause a reduction in viability with longer exposure times. Thus, the toxicity observed in C3 and D2 SWNT samples could be significant in pharmacological applications where doses are lower but exposure times are longer.

There are conflicting results in the literature on whether carboxylated SWNTs are cytotoxic. For example, Porter et al.[23] and Heister et al.[30] reported no significant cytotoxicity with carboxylated SWNT dispersions, but did not test concentrations above 10 μg/mL. In contrast, Saxena et al.[32] and Liu et al.[33] did find cytotoxicity with carboxylated SWNTs. The disagreement in the cytotoxicity of carboxylated SWNTs may stem from variations in the amounts of toxic contaminants residing in various carboxylated SWNT preparations as well as differences in assay details, such as the exposure times and concentrations tested. Note that potentially toxic residual metal catalysts are not likely to be the source of toxicity in our SWNT preparations because metal ions detected by ICP-MS analysis were below known toxic levels.

One possible explanation for the difference in cytotoxicity of pristine and carboxylated SWNTs is that the carboxylated SWNTs are better taken up by cells than noncarboxylated material, offering more potential for interference in cell function. For example, carboxylation often shortens SWNTs, and shorter SWNTs are better internalized by cells than longer SWNTs.[34,35] However, we directly observed the accumulation of both noncarboxylated and carboxylated SWNTs inside cells by Raman spectroscopy. Moreover, we compared the total amount of material taken up by NRK cells after 3 days incubation in either C2- or C3-SWNT dispersions at 100 μg/mL and found no significant difference between the two preparations. Since the C2 material is not toxic, but C3 is, a difference in SWNT uptake cannot account for the difference in cytotoxicity between noncarboxylated and carboxylated SWNTs.

Acid treatments to carboxylate SWNTs are known to generate nontubular carbon species that are byproducts of oxidation.[28−30] Thus, it was possible that the toxic material in the carboxylated SWNTs was not the SWNTs themselves, but carbon species produced by oxidation. To test this, the SWNTs were filtered to separate the larger SWNTs from smaller material. Raman spectroscopy demonstrated that the filtrate passing through the membrane had a larger D to G band ratio, evidence that amorphous carbons were removed from the larger SWNTs retained on the filter. AFM analysis validated this conclusion. To our knowledge, amorphous carbon fragments in SWNT preparations have not been previously reported as cytotoxic. Note, however, that our data does not directly prove that the heterogeneous amorphous carbons are the toxic species, only that the cytotoxic activity could be separated from intact SWNTs and copurified with small carbon fragments that had Raman signatures characteristic of amorphous carbon species.

Carboxylated SWNTs are more water-soluble than pristine SWNTs and have carboxyl functionalities for covalently attaching drugs and targeting agents. These properties have made carboxylated SWNTs the choice for many potential applications in drug development. Moreover, recent work has demonstrated that carboxylated SWNTs are biodegraded by myeloperoxidase,[36] an important consideration for *in vivo* applications. The findings reported here that dispersions of carboxylated SWNTs are more cytotoxic than dispersions of noncarboxylated material, and that the cytotoxic activity can be removed by filtration, are important in the future development of carboxylated SWNTs for pharmacological purposes.

CONCLUSIONS

Of nine different commercially available SWNT preparations dispersed under standard conditions, only two were significantly cytotoxic. Surprisingly, both of the cytotoxic SWNT samples had been functionalized by carboxylation. The cytotoxic material was

removed from the carboxylated SWNTs and copurified with heterogeneous small amorphous carbon species in the filtration process. This work suggests that carboxylated SWNT preparations under development for various pharmacological functions should be assessed for the presence of potentially toxic small carbon fragments.

MATERIALS AND METHODS

SWNT Materials. SWNT powders of different types were purchased from four different manufacturers coded A, B, C, and D in Table 1. ***CAUTION:*** *A particulate respirator should be worn when handling dry SWNT powders.* SWNT material A1, as described by manufacturer A, is produced by the cobalt−molybdenum catalytic chemical vapor deposition (CVD) process and is purified by the manufacturer to have a carbon content of >90% by weight (Table 1). Purified material A2 is described to contain >90% semiconducting SWNTs of which >50% are *(6,5)* SWNT structures. Purified material A3 has a high electrical conductivity and contains >50% *(7,6)* SWNTs. SWNT material B1 is the raw, as-prepared soot from a high-pressure carbon monoxide process and is reported by manufacturer B to contain >65% SWNTs and 15−35% metals by weight. SWNT material C1 is the raw, as-prepared soot produced by an electric arc discharge method and is reported by manufacturer C to have a carbonaceous purity of 40−60% and a metal content of ∼30% by weight. SWNT material C2 is purified by air oxidation and acid treatment and is described to have a carbonaceous purity of >90% and a metal content of 4−7% by weight. SWNT material C3 was carboxylated using nitric acid and, according to the manufacturer, has a carbonaceous purity of >90%, a metal content of 5−8% by weight, and contains 1.5−3.0 atom % of carboxylic acid groups. SWNT material D1 is produced by a CVD method and is purified by manufacturer D to contain >95% SWNTs by weight. SWNT material D2 is carboxylated with nitric and sulfuric acids and is described to contain >95% SWNTs, 2−7 wt % of carboxylic acid groups, and possibly other chemical functionalities such as hydroxyl groups.

Tissue Culture and Other Materials. Dulbecco's modified Eagle medium (DMEM) and trypsin were purchased from Gibco. Fetal bovine serum (FBS) was purchased from HyClone (Logan, UT). All other chemicals were purchased from Sigma Aldrich and were used as received.

Preparation of SWNT Dispersions. The bath sonication/centrifugation procedure used to prepare SWNT dispersions is summarized in Scheme 1. Stable dispersions of SWNTs were prepared in a biocompatible solution by dispersing 10 mg of as-received SWNT powder in 10 mL of 10 mM HEPES and 10 mg/mL BSA solution at pH 7.4 (HEPES/BSA). HEPES buffer is commonly used in cell culture media and is added in the solution to maintain neutral pH. BSA is the most abundant protein in blood serum and is used as surfactant to stabilize dispersed SWNTs in physiological aqueous environments.[37,38] Glass vials containing SWNT powders and HEPES/BSA solution were immersed in an ultrasonic bath unit (Elma T490DH) that operates at 120 W power and 40 kHz frequency for 4 h. Multiple SWNT dispersions could be prepared in separate glass vials simultaneously. The temperature of the bath was kept below 15 °C by using a cooling coil connected to a refrigerated water bath circulator (Isotemp 1006S) and by refilling the bath with ice-cold water at 30 min intervals. The sonication step was followed by two rounds of centrifugation to remove metal catalysts, SWNT bundles, and other heavy impurities. The first centrifugation was performed at 20000*g* for 5 min, and the supernatant was subjected to another centrifugation for 30 min at the same speed. The second supernatant was collected and stored at 4 °C. The SWNT dispersions were stable for up to three months with no visibly detectable precipitate.

Absorption Spectroscopy. Absorption spectra of SWNT dispersions were acquired using a dual-beam Perkin-Elmer Lambda 900 UV−vis−NIR spectrophotometer. All background-corrected spectra were acquired at a scan speed of 250 nm/min with a 0.24 s integration time.

Quantification of SWNTs in Dispersions or Cell Lysates by SDS−PAGE. The amount of SWNTs and related carbonaceous material in dispersions or cell lysates was determined using a modification of the sodium dodecyl sulfate polyacrylamide gel electrophoresis (SDS−PAGE) we described previously.[27] The modification was to use only a 10% running gel, omitting the 4% stacking gel described previously. This extended the range of carbon species retained by the gel at the interface between the gel and the running buffer to smaller structures. Briefly, a 10% SDS polyacrylamide gel was prepared using a Hoefer Mini Vertical Gel Caster for 10 × 8 cm plates with 1.5 mm thick spacers and 10-well combs. SWNT suspensions, dispersion samples, or cell lysates were mixed with 2× SDS sample loading buffer to a final concentration of 2% SDS and 5% 2-mercaptoethanol, and boiled for 3 min to reduce the disulfide bonds in proteins. Samples were subsequently loaded into the wells of the gel and an electric current was applied at a constant 100 V for 2 h. Following electrophoresis, optical images of gels were acquired using a 16-bit flatbed scanner (Visioneer 9520 photo scanner) at a resolution of 800 DPI. The concentrations of SWNT and related materials from dispersions or cell lysates were estimated from the pixel intensity based on the calibration curve prepared with SWNT suspensions of known concentrations.

When SDS−PAGE was used to quantify total C2 or C3 SWNT material in cell lysates, the cellular protein content in the lysates was determined by BCA assay and the volumes of the cell lysates applied to each well were adjusted so that the amount of protein was the same in each well. The average cellular protein content in a cell was calculated by dividing the total protein amount by the total number of cells in a cell culture dish. Once the amounts of C2 or C3 materials in cell lysates were determined by the SDS−PAGE method, the average amount of C2 or C3 materials per cell was calculated using the amount extracted divided by the total number of cells in a dish. Data from three independent experiments, with duplicate samples of each, were acquired, and the averages and standard deviations were calculated. The average protein content in a cell for the control, C2-, and C3-SWNT dispersion treated cells were 119.7 ± 14.5, 101.2 ± 9.9, and 109.8 ± 8.6 pg/cell, respectively. The average C2 and C3 materials extracted from a cell were 555.6 ± 60.6 and 548 ± 100.7 fg/cell, respectively, and the background level in the control cells was 37.3 fg/cell.

Elemental Analyses. Elemental analyses of aqueous SWNT dispersions were performed using a ThermoElectron X-Series inductively coupled plasma mass spectrometer. Samples (100 μL of SWNT dispersions, standards, and controls) were acid digested using a protocol developed in association with PreciLab Inc. (Addison, TX) as described previously.[27] Metals (Fe, Ni, Y, Mo, and/or Co) detected in all SWNT dispersions were below toxic levels for each respective metal.

Atomic Force Microscopy (AFM). AFM images were acquired under ambient conditions using a Nanoscope III multimode scanning probe microscope (Bruker AXS). The images were taken in the TappingMode with a "J" piezoelectric scanner and etched silicon probes (MPP-12100-W, Veeco) having a cantilever force constant of 5 N m^{-1} and an average resonant frequency of 180 kHz. Calibration of the scanner with 5% allowed tolerance was completed using a NanoDevices, Inc. standard. The height calibration was verified using muscovite mica etched with hydrofluoric acid.

The C2-SWNT and C3-SWNT dispersions, the C3 filtrate, and C3 SWNTs recovered from the filter were diluted 1:50 using deionized water and spun-cast onto freshly cleaved muscovite mica (Asheville-Schoonmaker Mica, Inc.). The C3-SWNT dispersion sample was spun-cast (Laurell, model WS-200-4NPP/RTV) at 1000 rpm for 60 s, whereas the C2-SWNT dispersion sample was spun-cast at 1500 rpm for 60 s. The D2-SWNT dispersion sample was spun-cast neat onto freshly cleaved mica at 3500 rpm for 30 s. Each sample was allowed to dry in a desiccator for 24 h prior to imaging. Length analysis was performed on 5 × 5 or 10 × 10 μm images and diameter analysis was performed on 2 × 2 μm images, using Nanoscope software.

X-ray Photoelectron Spectroscopy (XPS). XPS analyses of filtered materials were performed by Evans Analytical Group (Austin, TX) using a PHI Quantum 2000 spectrometer with monochromatic X-rays (1486.6 eV) operating at 20 W. The electron takeoff angle was 45°, and the analysis area was a 1 mm^2 spot. The binding energies were corrected by reference to the C1s line at 284.5 eV, and spectra were fitted using Multipak software from Physical Electronics.

Cell Culture. Normal rat kidney (NRK) cells were obtained from the American Type Culture Collection (Manassas, VA) and cultured in DMEM supplemented with 3.7 mg/mL sodium bicarbonate and 10% (v/v) FBS in a 37 °C incubator with 90% air and 10% CO_2. To determine the number of cells in a given sample, cells grown in tissue culture dishes were first detached using 0.05% (w/v) trypsin. Aliquots of these cell suspensions were diluted in an isotonic solution (Isoton II), and the number of cells was measured using a Beckman Coulter particle counter (Miami, FL).

Extracting SWNTs from Cells. Following incubation, cells were washed twice with DMEM and twice with PBS before being detached from the dish with trypsin. The suspended cells were collected by gentle centrifugation at 60*g* for 7 min and resuspended in PBS. An aliquot (5%) of the cell suspension was removed and the number of cells was determined using a Beckman Coulter particle counter. The remaining cells in suspension were collected by a second centrifugation. Cells in the pellet were lysed by resuspending them in a lysis buffer containing 1% SDS, 1 mM $MgCl_2$, and 1 mM $CaCl_2$ for 2 h in a 60 °C water bath. Subsequently, the cell lysate was treated with DNase I (0.1 μg/μL) for 2 h at 37 °C to degrade released DNA and reduce the viscosity of the lysate prior to analyzing the samples by SDS−PAGE.

Protein Assays. The total cellular protein content in cell lysate samples was determined using a microplate BCA protein assay kit (Pierce Chemical, Rockford, IL). Aqueous BSA standards at concentrations ranging from 0 to 1000 μg/mL were prepared from a 2.0 mg/mL BSA stock solution provided in the kit. In brief, 10 μL of diluted cell lysate samples and standards were dispensed into a 96-well microtiter plate followed by the addition of 200 μL of the BCA reagent. The microtiter plate was covered and incubated at 37 °C for 30 min. The plate was cooled to room temperature before the absorbance at 562 nm was measured using a BioTek Synergy 2 Multi-Mode microplate reader (Winooski, VT). The protein concentration of each sample was determined using the best-fit curve from the calibration plot created using the BSA standards.

Confocal Raman Spectroscopy. All Raman images and spectra were acquired with a WITec *alpha300* confocal Raman microscope system equipped with a 532 nm laser as the excitation source. Wavenumber calibration was performed using the 520.5 cm^{-1} line of a silicon wafer with a spectral resolution of ~1 cm^{-1}. The power density of the laser was measured using a Newport model-1918-C power meter with an 818-SL photodetector. Raman spectra were acquired directly from SWNT dispersions placed in 35 mm glass bottom "imaging" dishes (MatTek, Ashland, MA) or acquired from 50 μL drops of dispersions air-dried on glass slides. The laser was adjusted to a power density of 10 mW/cm^2 and focused using a 100× objective lens. The typical integration time was 0.1 s with 20 accumulation cycles. Duplicate samples were prepared from each SWNT dispersion and a minimum of three scans were acquired from each sample. LabSpec 5 software was used for background subtraction and peak area intensity integration of the scans. All spectra were plotted as the average of six scans.

To prepare for confocal Raman image scanning, NRK cells grown on glass coverslips were incubated with media containing various SWNT dispersions at a concentration of 100 μg/mL for 1 or 2 days. For lysosomal localization experiments, sucrose was added to the media at a final concentration of 0.12 M during the last 24 h. The cells were washed with PBS and incubated in fresh media with neither SWNT dispersion nor sucrose for 30 min at 37 °C and the chase was repeated once more. Finally, the cells were fixed with 4% paraformaldehyde, rinsed with PBS and water, and air-dried. Raman scan images were acquired over a 50 × 40 μm area using a 100× objective lens and a laser power density of around 10 mW/cm^2. The spectra were acquired at 0.5 μm intervals in both *x*- and *y*-directions with a 0.04 s integration time for each spectrum (total of 8000 spectra per image). The relative abundance of SWNTs in the scanned area was indicated by the integrated Raman G-band (1460−1700 cm^{-1}) intensities from each of the 8000 spectra using WITec image analysis software.

Cytotoxicity Assays. NRK cells (4×10^3 per well) were plated into 48-well plates in DMEM medium with 10% FBS and incubated at 37 °C for 24 h. The SWNT dispersions to be tested and HEPES/BSA solution (as a control) were diluted 1:1 with 2× concentrated DMEM that contained 20% FBS and the antibiotics penicillin (200 U/mL), streptomycin (0.2 mg/mL) and amphotericin B (5 μg/mL). Note that the final concentration of the HEPES/BSA solution or the SWNT dispersion was reduced by half after dilution. To start the experiment, the media was replaced with the control or SWNT containing media and the cells were incubated at 37 °C for 3 days. At the end of the incubation time, the cells were washed 3 times with PBS. To determine the number of cells in a well, 0.2 mL of 0.05% (w/v) trypsin was added to the well and the entire cell suspension was transferred into 10 mL of Isoton II for counting with the Coulter particle counter. To determine the total amount of nucleic acid in a well, 200 μL of 0.1% crystal violet in 10% ethanol (w/v) was added to each well and the plate was rocked for 20 min. Excess crystal violet was washed away with water, and the stain in the cells was extracted for 20 min with 200 μL of 10% acetic acid. A

volume of 180 μL of each extract was transferred to a corresponding well in a 96-well plate. The absorbance of each extract was read at 590 and 700 nm with a microplate reader (BioTek SynergyMx). The background absorbance at 700 nm was subtracted from that at 590 nm. The data for each experimental point was the average from 4 wells, and the data was expressed as a percent with the control set at 100%. All assays were performed in triplicate.

Filtration of SWNT Dispersions. A schematic description of the filtration procedure is shown in Scheme 2. The carboxylated C3-SWNT dispersion prepared in HEPES/BSA solution was diluted with HEPES/BSA solution to a concentration of 200 μg/mL. Five milliliters of the diluted SWNT dispersion was loaded in a 10 mL syringe with a 0.22 μm pore size disposable PVDF filter unit (Millex-GV) attached to the end. The dispersion was pushed gently through the filter. SWNT material that was too large to pass through the pores was retained on the filter and separated from smaller sized material collected in the filtrate. After the filtrate was collected, 5 mL of HEPES/BSA was added to the syringe and allowed to pass through the same filter to wash off any remaining small material left on the filter. The washing solution was collected in a separate tube. After the washing was completed, the SWNT material retained on the filter was recovered by drawing 3 mL of fresh HEPES/BSA solution up through the filter unit into the syringe. The recovered material in the syringe was transferred to a glass vial and redispersed for 30 min by bath sonication.

AUTHOR INFORMATION

Corresponding Author

*The University of Texas at Dallas, Department of Molecular and Cell Biology, 800 West Campbell Road, Richardson, TX 75080. E-mail: draper@utdallas.edu. Tel: 972-883-2512. Fax: 972-883-2409.

Notes

R.K.D. is a cofounder of Medical Nanotechnologies, Inc., and is the PI on an NIH STTR grant awarded jointly to the company and the University of Texas at Dallas.

ACKNOWLEDGMENT

The authors thank the SEMATECH/Semiconductor Research Corporation (Grant ERC425-027), the National Institute of Environmental Health Sciences STTR Program (Grant 1R41ES018002-01) and the UT Dallas Center for Applied Biology for supporting this work. We also thank Austin Swafford for help in developing atomic force microscopy methods.

REFERENCES

(1) Baughman, R. H.; Zakhidov, A. A.; de Heer, W. A. Carbon nanotubes—the route toward applications. *Science* **2002**, *297*, 787–792.

(2) Dresselhaus, M. S.; Dresselhaus, G.; Avouris, P. *Carbon nanotubes: synthesis, structure, properties, and applications*; Springer: New York, 2001; Vol. 80, p 447.

(3) Paradise, M.; Goswami, T. Carbon nanotubes—Production and industrial applications. *Mater. Des.* **2007**, *28*, 1477–1489.

(4) Liu, Z.; Tabakman, S.; Welsher, K.; Dai, H. Carbon Nanotubes in Biology and Medicine: In vitro and in vivo Detection, Imaging and Drug Delivery. *Nano Res.* **2009**, *2*, 85–120.

(5) Plata, D. L.; Gschwend, P. M.; Reddy, C. M. Industrially synthesized single-walled carbon nanotubes: compositional data for users, environmental risk assessments, and source apportionment. *Nanotechnology* **2008**, *19*, 1–14.

(6) Freiman, S.; Hooker, S.; Migler, K.; Arepalli, S. *NIST Recommended Practice Guide, Special Publication 960−19: Measurement Issues in Single Wall Carbon Nanotubes*; National Institute of Standards and Technology: Gaithersburg, MD: 2008; pp 1−78.

(7) Firme, C. P., III; Bandaru, P. R. Toxicity issues in the application of carbon nanotubes to biological systems. *Nanomedicine* **2010**, *6*, 245–256.

(8) Shvedova, A. A.; Kisin, E. R.; Porter, D.; Schulte, P.; Kagan, V. E.; Fadeel, B.; Castranova, V. Mechanisms of pulmonary toxicity and medical applications of carbon nanotubes: Two faces of Janus? *Pharmacol. Ther.* **2009**, *121*, 192–204.

(9) Liu, Z.; Chen, K.; Davis, C.; Sherlock, S.; Cao, Q.; Chen, X.; Dai, H. Drug delivery with carbon nanotubes for in vivo cancer treatment. *Cancer Res.* **2008**, *68*, 6652–60.

(10) Kostarelos, K. The long and short of carbon nanotube toxicity. *Nat. Biotechnol.* **2008**, *26*, 774–776.

(11) Shvedova, A. A.; Kagan, V. E. The role of nanotoxicology in realizing the 'helping without harm' paradigm of nanomedicine: lessons from studies of pulmonary effects of single-walled carbon nanotubes *J. Intern. Med.* **2010**, *267*, 106–118.

(12) Casey, A.; Herzog, E.; Lyng, F. M.; Byrne, H. J.; Chambers, G.; Davoren, M. Single walled carbon nanotubes induce indirect cytotoxicity by medium depletion in A549 lung cells. *Toxicol. Lett.* **2008**, *179*, 78–84.

(13) Warheit, D. B.; Laurence, B. R.; Reed, K. L.; Roach, D. H.; Reynolds, G. A.; Webb, T. R. Comparative Pulmonary Toxicity Assessment of Single-wall Carbon Nanotubes in Rats. *Toxicol. Sci.* **2004**, *77*, 117–125.

(14) Lam, C. W.; James, J. T.; McCluskey, R.; Hunter, R. L. Pulmonary toxicity of single-wall carbon nanotubes in mice 7 and 90 days after intratracheal instillation. *Toxicol. Sci.* **2004**, *77*, 126–134.

(15) Itkis, M. E.; Perea, D. E.; Jung, R.; Niyogi, S.; Haddon, R. C. Comparison of analytical techniques for purity evaluation of single-walled carbon nanotubes. *J. Am. Chem. Soc.* **2005**, *127*, 3439–3448.

(16) O'Connell, M. J.; Boul, P.; Ericson, L. M.; Huffman, C.; Wang, Y. H.; Haroz, E.; Kuper, C.; Tour, J.; Ausman, K. D.; Smalley, R. E. Reversible water-solubilization of single-walled carbon nanotubes by polymer wrapping. *Chem. Phys. Lett.* **2001**, *342*, 265–271.

(17) Karajanagi, S. S.; Yang, H.; Asuri, P.; Sellitto, E.; Dordick, J. S.; Kane, R. S. Protein-assisted solubilization of single-walled carbon nanotubes. *Langmuir* **2006**, *22*, 1392–1395.

(18) Bahr, J. L.; Tour, J. M. Covalent chemistry of single-wall carbon nanotubes. *J. Mater. Chem.* **2002**, *12*, 1952–1958.

(19) Dresselhaus, M. S.; Jorio, A.; Hofmann, M.; Dresselhaus, G.; Saito, R. Perspectives on Carbon Nanotubes and Graphene Raman Spectroscopy. *Nano Lett.* **2010**, *10*, 751–758.

(20) Gillies, R. J.; Didier, N.; Denton, M. Determination of cell number in monolayer cultures. *Anal. Biochem.* **1986**, *159*, 109–113.

(21) Shi Kam, N. W.; Jessop, T. C.; Wender, P. A.; Dai, H. Nanotube molecular transporters: internalization of carbon nanotube-protein conjugates into Mammalian cells. *J. Am. Chem. Soc.* **2004**, *126*, 6850–6851.

(22) Jin, H.; Heller, D. A.; Strano, M. S. Single-particle tracking of endocytosis and exocytosis of single-walled carbon nanotubes in NIH-3T3 cells. *Nano Lett.* **2008**, *8*, 1577–1585.

(23) Porter, A. E.; Gass, M.; Bendall, J. S.; Muller, K.; Goode, A.; Skepper, J. N.; Midgley, P. A.; Welland, M. Uptake of noncytotoxic acid-treated single-walled carbon nanotubes into the cytoplasm of human macrophage cells. *ACS Nano* **2009**, *3*, 1485–1492.

(24) Cohn, Z. A.; Ehrenreich, B. A. The uptake, storage, and intracellular hydrolysis of carbohydrates by macrophages. *J. Exp. Med.* **1969**, *129*, 201–225.

(25) Silverstein, S. C.; Steinman, R. M.; Cohn, Z. A. Endocytosis. *Annu. Rev. Biochem.* **1977**, *46*, 669–722.

(26) Dresselhaus, M. S.; Dresselhaus, G.; Saito, R.; Jorio, A. Raman spectroscopy of carbon nanotubes. *Phys. Rep.* **2005**, *409*, 47–99.

(27) Wang, R.; Mikoryak, C.; Chen, E.; Li, S.; Pantano, P.; Draper, R. K. Gel Electrophoresis Method to Measure the Concentration of Single-Walled Carbon Nanotubes Extracted from Biological Tissue. *Anal. Chem.* **2009**, *81*, 2944–2952.

(28) Worsley, K. A.; Kalinina, I.; Bekyarova, E.; Haddon, R. C. Functionalization and Dissolution of Nitric Acid Treated Single-Walled Carbon Nanotubes. *J. Am. Chem. Soc.* **2009**, *131*, 18153–18158.

(29) Rinzler, A. G.; Liu, J.; Dai, H.; Nikolaev, P.; Huffman, C. B.; Rodriguez-Macias, F. J.; Boul, P. J.; Lu, A. H.; Heymann, D.; Colbert, D. T.; Lee, R. S.; Fischer, J. E.; Rao, A. M.; Eklund, P. C.; Smalley, R. E. Large-scale purification of single-wall carbon nanotubes: process, product, and characterization. *Appl. Phys. A: Mater. Sci. Process.* **1998**, *67*, 29–37.

(30) Heister, E.; Lamprecht, C.; Neves, V.; Tilmaciu, C.; Datas, L.; Flahaut, E.; Soula, B.; Hinterdorfer, P.; Coley, H. M.; Silva, S. R.; McFadden, J. Higher dispersion efficacy of functionalized carbon nanotubes in chemical and biological environments. *ACS Nano* **2010**, *4*, 2615–2626.

(31) Worle-Knirsch, J. M.; Pulskamp, K.; Krug, H. F. Oops they did it again! Carbon nanotubes hoax scientists in viability assays. *Nano Lett.* **2006**, *6*, 1261–1268.

(32) Saxena, R. K.; Williams, W.; McGee, J. K.; Daniels, M. J.; Boykin, E.; Ian Gilmour, M. Enhanced in vitro and in vivo toxicity of poly-dispersed acid-functionalized single-wall carbon nanotubes. *Nanotoxicology* **2007**, *1*, 291–300.

(33) Liu, D.; Yi, C.; Zhang, D.; Zhang, J.; Yang, M. Inhibition of Proliferation and Differentiation of Mesenchymal Stem Cells by Carboxylated Carbon Nanotubes. *ACS Nano* **2010**, *4*, 2185–2195.

(34) Becker, M.; Fagan, J.; Gallant, N.; Bauer, B.; Bajpai, V.; Hobbie, E.; Lacerda, S.; Migler, K.; Jakupciak, J. Length-Dependent Uptake of DNA-Wrapped Single-Walled Carbon Nanotubes. *Adv. Mater.* **2007**, *19*, 939–945.

(35) Jin, H.; Heller, D. A.; Sharma, R.; Strano, M. S. Size-Dependent Cellular Uptake and Expulsion of Single-Walled Carbon Nanotubes: Single Particle Tracking and a Generic Uptake Model for Nanoparticles. *ACS Nano* **2009**, *3*, 149–158.

(36) Kagan, V. E.; Konduru, N. V.; Feng, W.; Allen, B. L.; Conroy, J.; Volkov, Y.; Vlasova, I. I.; Belikova, N. A.; Yanamala, N.; Kapralov, A.; Tyurina, Y. Y.; Shi, J.; Kisin, E. R.; Murray, A. R.; Franks, J.; Stolz, D.; Gou, P.; Klein-Seetharaman, J.; Fadeel, B.; Star, A.; Shvedova, A. A. Carbon nanotubes degraded by neutrophil myeloperoxidase induce less pulmonary inflammation. *Nat. Nanotechnol.* **2010**, *5*, 354–359.

(37) Edri, E.; Regev, O. pH effects on BSA-dispersed carbon nanotubes studied by spectroscopy-enhanced composition evaluation techniques. *Anal. Chem.* **2008**, *80*, 4049–4054.

(38) Elgrabli, D.; Abella-Gallart, S.; Aguerre-Chariol, O.; Robidel, F.; Rogerieux, F.; Boczkowski, J.; Lacroix, G. Effect of BSA on carbon nanotube dispersion for *in vivo* and *in vitro* studies. *Nanotoxicology* **2007**, *1*, 266–278.